Oikos **xx** *(2018) xx-xx*
doi:10.1111/oik.05041
a Malthusian Relativity paper

$\iota^{**}=7/3\psi$
mrLife.org

The natural selection of metabolism explains curvature in allometric scaling

Lars Witting
Greenland Institute of Natural Resources, Box 570, DK-3900 Nuuk, Greenland

Abstract I simulate the natural selection of metabolism and mass to explain the curvature in the metabolic allometry for placental and marsupial mammals. The simulation model starts with a single ancestor in each clade at the Cretaceous-Palaeogene boundary 65 million years ago. The release of inter-specific competition by the extinction of dinosaurs make it possible for each clade to diversify into a multitude of species across a wide range of empty niches. The selection of mass in these species depends on the net assimilated energy that depends on *i*) the handling of the resources in the different niches, and on *ii*) mass-specific metabolism that defines the pace of the handling process. The model is fitted to explain the maximum observed body masses over time and the current inter-specific allometry for metabolism. The selection of mass-specific metabolism is found to bend the metabolic allometry over time, even when all species have the same selection on the per-generation time-scale of natural selection. This is because the smaller species evolve over a larger number of generations than the larger species. The strongest curvature is in the placental clade, where the estimated rate of exponential increase in mass-specific metabolism is 9.3×10^{-9} (95% CI: 7.3×10^{-9} - 1.1×10^{-8}) on the per-generation time-scale. This is an order of magnitude larger than the estimate for marsupials, in agreement with an average metabolism that is 30% larger in placentals relative to marsupials of similar size.

Keywords: Evolution, natural selection, metabolism, body mass, allometry, curvature

1 Introduction

The existence of an inter-specific allometry between metabolism and mass indicates that the two traits evolve as an energetic balance. The natural selection of mass may depend on the selection of metabolism, just as the selection of metabolism may dependent on the selection of mass.

The latter is the usual assumption in allometric studies. Empirical analyses treat metabolism as the dependent parameter on double logarithmic plots of metabolism on mass (Kleiber 1932; Peters 1983; Calder 1984; Savage et al. 2004; McNab 2008; White et al. 2009). And traditional allometric theory explains metabolism as a trait that is adapted to mass, by a physiology where branching networks are optimised to supply the mass with energy for metabolism (West et al. 1997, 1999a,b; Banavar et al. 1999; Dodds et al. 2001; Dreyer and Puzio 2001; Rau 2002; Santillán 2003; Glazier 2010). This view is extended in the Metabolic theory of ecology (MTE) to include ecological processes that reflect the physical and kinetic constraints on metabolism (Gillooly et al. 2002; Brown et al. 2004; Sibly et al. 2012; Humphries and McCann 2014).

While biology will obey the constraints of physics and biochemistry, it is the primary selection of metabolism and mass that explains the evolution of large species with metabolic rates. Yet, the allometric component of MTE does not include any primary selection of metabolism and mass. MTE is instead recognising natural selection in separate models on the evolution of mass and other life histories (Brown and Sibly 2006; Bueno and López-Urrutia 2012). These have, however, not yet reconciled the observed allometries with the selected mass, as the frequency-independent selection of Brown and Sibly (2006) does not allow for a realistic decline in the rate of population dynamic growth (r), and carrying capacity (n^*), with a selected increase in mass (Witting 2017b).

The observed inter-specific decline in r and n^* with an increase in mass (Fenchel 1974; Damuth 1981, 1987) requires a frequency-dependent selection of mass (Simpson 1953; Dawkins and Krebs 1979; Parker 1979, 1983; Haigh and Rose 1980; Maynard Smith and Brown 1986; Vermeij 1987; Witting 2000). One example is the density-frequency-dependent selection in the theory of Malthusian relativity, where the exponents of body mass allometries are selected by the primary selection of metabolism and mass (Witting 1995, 1997, 2008, 2017a,b).

Malthusian Relativity describes the selection and flow of energy in the population, starting with the assimilation of resources by individuals. The net energy that is available for reproduction drives the population dynamics growth, which is subject to density-

dependent regulation by mechanisms of interactive competition between the individuals in the population. The interactive competition implies that the larger than average individuals will tend to monopolise the assimilation of resources, and this creates a bias in net energy that will increase with an increase in the abundance and level of interference competition in the population.

This density-frequency-dependent bias in net energy selects for an increase in average mass, but the physiology selects for a decline by a quality-quantity trade-off (Smith and Fretwell 1974; Stearns 1992), where parents can produce many small, or a few large, offspring from the same amount of energy. The selection of mass is thus dependent on a sufficiently high level of interactive competition. And this is guaranteed by a population dynamic feed-back, where a potential selection decline in mass is strengthening the selection of mass, as the abundance and level of interfere is increasing by the extra population growth that is induced with a selection decline in average mass. The resulting selection attractor is driven by the average net energy, with an unconstrained selection for an exponential increase in net energy generating persistent density-frequency-dependent selection for an exponential increase in mass (Witting 1997, 2003). A schematic illustration of the feed-back selection is shown in Fig. 1, with further details given by Witting (2017a,b).

The selection of net energy is dependent on inter-specific interaction, where the competitive exclusion of smaller species by the interactive competition with larger species is likely to restrict the net energy that is available for the smaller species. The result is a species distribution of net energy, where it is only the larger species in competitive guilds that are expected to have unconstrained selection on net energy and mass. Yet, the intra-specific selection of mass in all the species is driven by the same underlying mechanism, with the species distribution of masses evolving primarily from the underlying distribution of net energy across species.

The intra-specific selection of mass involves a mass-rescaling selection that dilates the time-scale of natural selection by a decline in mass-specific metabolism (Fig. 1, inner loop; see Witting 2017a for details). This ensures that the net assimilated energy is constant on the per-generation time-scale of natural selection when additional mass is selected, as it is required by the population dynamic feed-back selection that is driven by the net assimilated energy.

This mass-rescaling selects exponents of inter-specific allometries from a log-linear scaling between the life history and mass (Witting 2017a). The numerical values of the exponents follow primarily from the ecological constraints on the selected optimum of the density-dependent foraging that generates the net energy that is driving the selection of mass. The theoretically predicted exponents are thus dependent on the foraging behaviour in d-dimensional home ranges ($d \in \{1, 2, 3\}$), with the $-1/4$ exponent for mass-specific metabolism being the two-dimensional (2D) case of the more general $-1/2d$ (Witting 1995, 2017a).

Malthusian Relativity was originally proposed as one-sided, in the sense that it described the mass-rescaling

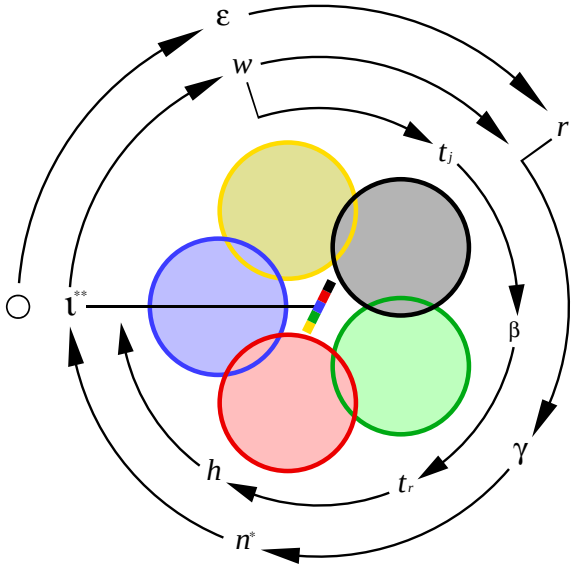

Figure 1: **The feed-back selection of mass.** A diagram of population dynamic feed-back selection, with symbols that relate to the population average, and coloured circles that symbolize individual home ranges in two-dimensional space with interactive competition in zones of overlap. Winners (dominating colour) monopolize resources, and this generates a body mass biased resource access that is proportional to the slope of the multi-coloured bar in centrum, with the invariant interference (ι^{**}) of the selection attractor determining the evolution of this bias. The black o to the left represents the origin of self-replication, and selection for an exponential increase in net energy (ϵ) maintains relatively high population dynamic growth (r) and continued feed-back selection for an exponential increase in mass. The attractor of the feed-back is given by the outer ring of symbols [r:population growth $\rightarrow$ γ:density regulation $\rightarrow$ n^*:population abundance $\rightarrow$ ι:interference level $\rightarrow$ w:selection on body mass $\rightarrow$ r:population growth]. Selection for a change in mass initiates the inner loop of mass-rescaling selection [w:mass change $\rightarrow$ t_j:juvenile period $\rightarrow$ β:metabolic rate $\rightarrow$ t_r:reproductive period $\rightarrow$ h:home range $\rightarrow$ ι:interference]. From Witting (2017b).

influence on metabolism from the primary selection of mass (Witting 1995, 1997), but not the selection influence on mass from the primary selection of metabolism. The former selection was well-suited for the prediction of typical allometries in multicellular animals, yet the exponents in unicellular animals have been found to extend beyond the predicted range. The exponent for mass-specific metabolism increases from the typical $-1/4$ in multicellular animals, over invariance in unicellular eukaryotes, to an apparent value around 0.84 in prokaryotes (Makarieva et al. 2005, 2008; DeLong et al. 2010; Witting 2017a).

A two-sided model with primary selection on metabolism and mass was recently developed to explain the larger range of allometries across the tree of life (Witting 2017a,b). The resource assimilation of an individual was extended into a product, where assimilation by a resource handling process was multiplied by the pace (or speed) of the process, with pace being proportional to the metabolic energy that is used on handling per unit mass. This product generates gross energy, and by defining the net energy that is available for reproduction as the difference between the gross energy and the total metabolism of the organism, Witting (2017a) found the mass-specific work of handling to be selected as mass-specific metabolism. This implies primary selection for an increase in mass-specific metabolism, an increase that generates part of the net energy that is a pre-condition for the selection of mass, and the associated secondary rescaling of mass-specific metabolism (Witting 2017a,b).

Malthusian Relativity predicts linear allometries from invariant selection responses, yet the most studied allometry (metabolism in mammals) is an upward bend curve (upward concave, i.e., convex curve), where the local exponent for total metabolism is increasing from smaller values around 0.67 to larger values of about 0.75 with an increase in mass (Hayssen and Lacy 1985; Dodds et al. 2001; Packard and Birchard 2008; Kolokotrones et al. 2010; MacKay 2011). A split of mammals into placentals and marsupials illustrates that the curvature is evident in placentals, but apparently not in marsupials (MacKay 2011). When two outliers are removed, the latter have an almost perfect Kleiber scaling with an estimated exponent of 0.75 ± 0.01 (MacKay 2011).

To examine for the selection of these curvatures in metabolic scaling, I use Malthusian Relativity with primary selection on metabolism and mass to simulate the evolution of placental and marsupial mammals over the past 65 million years. The predicted log-linear allometries for taxonomic clades of multicellular animals are dependent on the assumption that the major component of the body mass variation originates from primary variation in the handling and/or density of the underlying resources (Witting 2017a). This assumption may hold in many cases, at least as a first approximation, as it is reasonable to assume that a large fraction of the body mass variation is generated by the adaptation of species to resources in different niches.

But what happens over evolutionary time when this evolution comes to a halt because the resource handling processes of the species are becoming well-adapted to their niches? If there is no background evolution in mass-specific metabolism, we may expect a stationary distribution of body masses in the clade over time, as there should be no evolution in net energy and mass. But it is resource handling only that is selected towards an optimum for a given niche. With mass-specific metabolism being selected as the pace of the resource handling that generates net energy for reproduction and the selection of mass (Witting 2017a), we may always expect a certain positive background selection in mass-specific metabolism, net energy and mass. We can therefore expect no optimal mass for a species in a given niche, and this paper analyses whether the positive background selection of mass-specific metabolism and mass will explain the different degrees of curvature that are observed in the metabolic allometry for placental and marsupial mammals.

2 The selection model

To simulate the natural selection of a distribution of mammal species that differ in metabolism and mass, I simulate the evolution of placental and marsupial mammals from the extinction of the dinosaurs at the Cretaceous-Palaeogene (K-Pg) boundary 65 million years ago (MA). This involves a simplified two-step model for each of the clades, with each clade having a single ancestor at 65 MA. The first component of the model makes the ancestor of a clade diversify into a multitude of evolutionary lineages (species) in the empty niches at the K-Pg boundary, and the other component is selecting the metabolism and body mass of each of the evolutionary lineages within a clade over time.

Primary selection for an increase in net energy is selecting for the exploitation of the more resource-rich niches. And with speciation between populations in different niches, the competitive exclusion by inter-specific interactions will create a distribution of species across niches. Species in the resource-rich niches are selected for a higher net energy over time, while species that are

excluded into resource-sparse niches may experience a decline in net energy.

2.1 The selection of net energy

I use the life history and selection model in Witting (2017a,b) to describe the evolution of metabolism, net energy, and mass in a species. It is fitness costly to burn energy in metabolism, and we do therefore expect that metabolism is optimised by natural selection to reflect the physiological and ecological work that is essential for the selected life history. A perfect metabolic efficiency is impossible to obtain, yet I will assume that the energetics of the physiology is optimised by natural selection. This allows me to study a life history evolution that is selected along an optimal fitness ridge that reflects a physiology that is optimised by natural selection, assuming implicitly that the optimal physiology is invariant of mass.

Net energy (ϵ, SI unit J/s) is defined here as the energy that is available for reproduction per unit physical time. It is given as a product $\epsilon = \alpha\tilde{\beta}$ between the resource handling process (α, SI unit J) and the pace ($\tilde{\beta}$, SI unit 1/s) of this process, with pace being selected as a proxy ($\tilde{\beta} = \beta/W$) of mass-specific metabolism (β, SI unit J/gs), where $W = 1$J/g is the mass-specific work that is carried out by metabolising one joule per gram of tissue (see Witting 2017a for the selection of these relationships).

For unconstrained selection, this implies primary selection for an exponential rate (r) of increase

$$r_\epsilon = \mathrm{d}\ln\epsilon/\mathrm{d}\tau \tag{1}$$

in the average net energy on the per-generation time-scale of natural selection (τ, time in generations), with the $\ln\epsilon$ notation being short for $\ln[\epsilon/(1\mathrm{J/s})]$. This increase is driven by an increase in the two sub-components of resource handling and mass-specific metabolism

$$r_\epsilon = r_\alpha + r_{\beta_\beta} = \mathrm{d}\ln\alpha/\mathrm{d}\tau + \mathrm{d}\ln\beta_\beta/\mathrm{d}\tau \tag{2}$$

with sub-script β denoting the pre-mass component that evolves from primary selection on metabolism independently of the natural selection of mass (i.e., excluding the mass-rescaling selection of metabolism that causes a decline in mass-specific metabolism and net energy in physical time to maintain constant mass-specific metabolism and net energy on the per-generation time-scale of natural selection).

While it is likely that there is a potential upper limit to the selection of mass-specific metabolism, I assume that all species are well below such a limit. This implies a steady unconstrained selection of mass-specific metabolism across all the species in a clade. The rate of increase (r_{β_β}) in the pre-mass component of mass-specific metabolism may thus be relatively similar on the per-generation time-scale of the different species. I do therefore, for simplicity, assume that all species evolve by the same r_{β_β}. This rate is then estimated separately for placentals and marsupials.

Resource handling ($\alpha = \grave{\alpha}\rho$) is given as a joint function of the actual (intrinsic) handling ($\grave{\alpha}$, SI unit $\mathrm{Jm^2/J}$) of the resource (ρ, SI unit $\mathrm{J/m^2}$) itself. A species on a stable resource is therefore selected towards an upper limit ($\alpha^{**} = \grave{\alpha}^{**}\rho$) that is given by an optimal intrinsic handling ($\grave{\alpha}^{**}$) of the relevant resources. A species that is excluded by inter-specific interactions into a resource-sparse niche will instead, most typically, experience a decline in α because of a decline in ρ. A third species that is evolving into a more resource-rich niche will typically experience an increase in both ρ and $\grave{\alpha}$. To capture this, I assume a linear trend

$$r_\alpha = (\alpha^{**} - \alpha)/c \tag{3}$$

where the rate of change in the resource handling of eqn 2 is proportional to the evolutionary distance from the optimum, with c being a clade specific constant. When a species is adapting to a new niche with more or less resource, we expect that the initial changes in the net energy that is obtained per handling cycle are large, and that the rate of change will decline as the species approached the optimum.

2.2 Life history selection

With the three equations above we can calculate the evolutionary changes in the net energy of the average individual in the population. It is this change in energy that is driving the natural selection of mass and the associated mass-rescaling of the life history (Witting 2017a,b). The increase in net energy is first allocated into reproduction. This generates population growth, and an increased abundance with a sustained interference competition that is selecting the energy into an increase in mass. The associated selection attractor is an evolutionary steady state, where net energy and mass are increasing exponentially while the level of interference competition is stable, and the population abundance is declining slowly in accordance with the predicted allometric scaling (Witting 1997, 2003).

The per-generation change in mass (w, SI unit g) at the evolutionary steady state is calculated from the rate of change in net energy ($\mathrm{d}\ln\epsilon/\mathrm{d}\tau$, eqn 1) by the

following formula

$$\begin{aligned} \ln w_{\tau+1} &= \ln w_\tau + \mathrm{d}\ln w/\mathrm{d}\tau \\ \mathrm{d}\ln w/\mathrm{d}\tau &= (\partial \ln w/\partial \ln \epsilon)(\mathrm{d}\ln \epsilon/\mathrm{d}\tau) \\ \partial \ln w/\partial \ln \epsilon &= 2d/(2d-1) \end{aligned} \quad (4)$$

where d is the ecological dimensionality of the foraging behaviour, and the log-linear selection relation $\partial \ln w/\partial \ln \epsilon = 2d/(2d-1)$ is the inverse of the exponent $\hat{\epsilon} = (2d-1)/2d$ for the theoretical allometry between net energy and mass (Witting 2017a), with $d = 2$ for the terrestrial mammals in this study.

The evolution of mass-specific metabolism is then given by the primary selection ($\mathrm{d}\ln \beta_\beta/\mathrm{d}\tau$) of eqn 2 and the mass-rescaling response of metabolism ($\mathrm{d}\ln \beta_w/\mathrm{d}\tau$) to the evolutionary changes in mass (Witting 2017a). Hence,

$$\begin{aligned} \ln \beta_{\tau+1} &= \ln \beta_\tau + \mathrm{d}\ln \beta/\mathrm{d}\tau \\ \mathrm{d}\ln \beta/\mathrm{d}\tau &= \mathrm{d}\ln \beta_\beta/\mathrm{d}\tau + \mathrm{d}\ln \beta_w/\mathrm{d}\tau \\ \mathrm{d}\ln \beta_w/\mathrm{d}\tau &= (\partial \ln \beta_w/\partial \ln w)(\mathrm{d}\ln w/\mathrm{d}\tau) \\ \partial \ln \beta_w/\partial \ln w &= -1/2d \end{aligned} \quad (5)$$

where $\partial \ln \beta_w/\partial \ln w = -1/2d$ is the linear selection relation of the theoretical mass-rescaling exponent for mass-specific metabolism.

To transfer these evolutionary trajectories that are calculated on the per-generation (τ) time-scale of natural selection into physical time ($t = \sum_{i\in\tau} t_{g,i}$; t:time in years; t_g:generation time in years), we need to calculate the per-generation changes in a generation time (t_g) that is measured in physical time. These changes

$$\begin{aligned} \ln t_{g,\tau+1} &= \ln t_{g,\tau} + \mathrm{d}\ln t_g/\mathrm{d}\tau \\ \mathrm{d}\ln t_g/\mathrm{d}\tau &= \mathrm{d}\ln t_{g,\beta}/\mathrm{d}\tau + \mathrm{d}\ln t_{g,w}/\mathrm{d}\tau \\ \mathrm{d}\ln t_{g,\beta}/\mathrm{d}\tau &= (\partial \ln t_{g,\beta}/\partial \ln \beta_\beta)(\mathrm{d}\ln \beta_\beta/\mathrm{d}\tau) \\ \mathrm{d}\ln t_{g,w}/\mathrm{d}\tau &= (\partial \ln t_{g,w}/\partial \ln w)(\mathrm{d}\ln w/\mathrm{d}\tau) \end{aligned} \quad (6)$$

are given by the mass ($\mathrm{d}\ln t_{g,w}/\mathrm{d}\tau$) and metabolic ($\mathrm{d}\ln t_{g,\beta}/\mathrm{d}\tau$) rescaling changes in generation time in response to the evolutionary changes in mass and the pre-mass component of mass-specific metabolism, where $\partial \ln t_{g,w}/\partial \ln w = 1/2d$ is the selection relation of the theoretical mass-rescaling exponent, and $\partial \ln t_{g,\beta}/\partial \ln \beta_\beta = -1$ is the rescaling of generation time in relation to the pre-mass evolution of mass-specific metabolism (Witting 2017a).

2.3 Mammalian evolution

To simulate the evolution of the inter-specific metabolic allometry for placental and marsupial mammals, I assume that the common ancestors were adapted to their niches prior to the Cretaceous-Palaeogene boundary at 65 MA (with $r_\alpha = 0$ and $\alpha = \alpha^{**}$). Following an estimate from O'Leary et al. (2013), I assume a common ancestor with a mass of 125 grams at 65 MA for placentals. This mass is about the same as the geometric mean of 146 grams across all placentals today (for the mass data of Pacifici et al. 2013). With a current average mass of 309 grams for all marsupials, I assume a 300 grams marsupial ancestor at 65 MA.

The generation times ($t_{g,65\mathrm{MA}}$) of the ancestors at 65MA were adjusted to predict a generation time of 3.3 years for a current placental mammal of 146 grams, and of 2.9 years for a current marsupial mammal of 309 grams. This coincides with the geometric means across all extant placentals and marsupials, as calculated from the body mass and generation time estimates of Pacifici et al. (2013). But the 2.9 years estimate for a 309 grams marsupial does not match well with an estimate of 3.3 years for an average placental of 146 grams. The average metabolism of a marsupial is only 77% of the metabolism of a similar sized placental (McNab 2008), and this suggests that marsupials should have a longer generation time than placentals. And with a 309 grams placental having an average generation time of 4.0 years, the corresponding allometric estimate for a 309 grams marsupial is 5.1 year. I use both the 2.9 and 5.1 years estimates as the target for marsupials.

Then, at 65 MA I created a set of hundred placental species that all resembled the 125 grams placental ancestor, and a set of 100 marsupial species that all resembled the 300 grams ancestor for marsupials. The species of each clade were set to diversify into niches that differed linearly in $\ln \alpha^{**}$ from a minimum ($\alpha^{**}_{\mathrm{min}}$) to a maximum ($\alpha^{**}_{\mathrm{max}}$). Initially at 65 MA, all marsupials, or placentals, had the same mass, metabolism and generation time, with these traits evolving by eqns 2 to 6 in per-generation time-steps as physical time progress.

Having the same initial metabolism, it is the potential maximum to resource handling ($\alpha^{**}_{\mathrm{max}}$) that allows for the evolution of the largest body mass in the set of species. Thus, for the evolutionary lineage with $\alpha^{**}_{\mathrm{max}}$, I would estimate $\alpha^{**}_{\mathrm{max}}$ and the c parameter of eqn 3 (c is constant across all the species in a clade) by least-squares fits of the resulting body mass trajectory to the global maximum body mass of terrestrial mammals for placentals, and to the maximum for South America for marsupials, with data obtained from Smith et al. (2010). By fitting these two parameters to the trajectory, I was able to simulate not only the evolution of the maximum observed mass, but also the evolution of the downward bend in the observed trajectories of maximum mass (see Fig. 3 and 4).

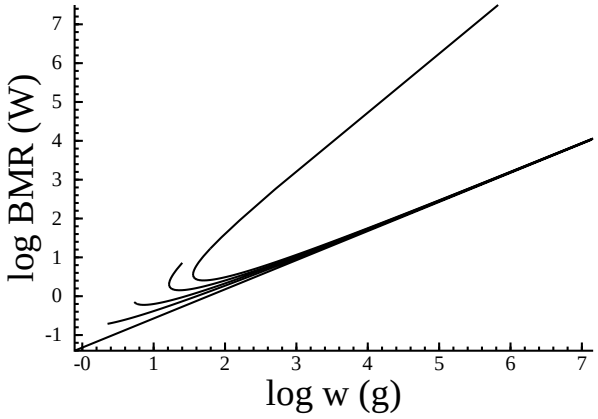

Figure 2: **The allometric bend.** The predicted unconstrained relationship between the basal metabolic rate (BMR) and body mass (w) for a mammalian like clade that has evolved for 65 million years. A straight allometric line with an exponent of 0.75 is expected only in the absence of primary selection on mass-specific metabolism ($r_{\beta_\beta} = 0$). The relationship is instead bend to an increasing degree with an increase in r_{β_β}, with the illustrated relationships representing a per-generation r_{β_β} of 0, 1×10^{-8}, 1.5×10^{-8}, 2.0×10^{-8}, and 2.4×10^{-8}.

The potential minimum to resource handling (α^{**}_{min}) was adjusted to hit a current minimum mass of 2.2 grams for placental and of 7 grams for marsupials. These values corresponds with the minimum masses in the McNab (2008) data that I used for the allometric relationship between metabolism and mass.

I could then, for different values of r_{β_β} and $\beta_{65\text{MA}}$, adjust the α^{**}_{min}, α^{**}_{max}, c and $t_{g,65\text{MA}}$ parameters as above, and simulate the species distributions over time. The distributions at 0MA were transformed by a linear interpolation into a predicted relationship between metabolism and mass, allowing r_{β_β} and $\beta_{65\text{MA}}$ to be adjusted to obtain the best least-squares fit between the predicted relationships and the allometric data from McNab (2008), with confidence intervals estimated by bootstraps of the data.

3 Results

In the absence of primary selection on metabolism ($r_{\beta_\beta} = 0$), the simulated relationship between metabolism and mass resemble Kleiber (1932) scaling, with a log-linear allometry, i.e., a scale-free power-law relationship, and a 3/4 exponent for the relationship between total metabolism and mass (Fig. 2).

With primary selection on metabolism ($r_{\beta_\beta} > 0$), it is especially the mass-specific metabolisms of the smaller species that increase over time. Although all the mammalian lineages in a simulation have the same rate of increase in mass-specific metabolism on the per-generation time-scale of natural selection, the increase is largest in the smaller species in physical time. This is because they, due to their smaller generation times from the mass-rescaling of the body mass evolution just after the Cretaceous-Palaeogene boundary, evolve over a larger number of generations than the larger species. Hence as the metabolic increase is selected into mass by eqns 2 and 4, we find that the left-hand side of the allometry is bending upward with respect to both metabolism and mass (Fig. 2).

For small rates of increase in metabolism, this creates an upward bend in the left-hand side of the allometry. For the larger rates of increase in Fig. 2, it creates the evolution of a separate branch of phylogenetic lineages with large body masses and increasingly high metabolic rates. This second branch has an allometric exponent of 3/2 for total metabolism and of 3/4 for mass-specific metabolism, and this corresponds with an analytically deduced exponent for lineages where $r_\alpha = 0$ and $r_{\beta_\beta} > 0$ (Witting 2016).

3.1 Placental mammals

The simulated span of body masses for placental mammals over the past 65 million years are shown in the top plot in Fig. 3 for the best estimate of the exponential increase in metabolism. The inter-specific metabolic allometries that follow from the simulation at 50MA, 30MA and 0MA are shown in the bottom plot together with the placental data at 0MA from McNab (2008).

The estimated allometry is bent by time due to the exponential increase in metabolism. Initially at 50MA, just after the evolutionary diversification into a multitude of niches, the evolutionary variation in body mass is selected predominantly from variation in the handling of the different resources. This produces a typical Kleiber allometry with almost no bend from primary variation in mass-specific metabolism. But the generation of body mass variation from evolution in resource handling comes to a stop over time, while the selected increase in metabolism continues to feed the natural selection of mass. This is affecting especially the smaller species that are selected over a larger number of generations, and this is apparent from the minimum mass in the top plot of Fig. 3. At first, it declines due to the competitive exclusion of the lineage into a resource-sparse niche. But after a while it begins to increase from the selection increase in mass-specific metabolism. The

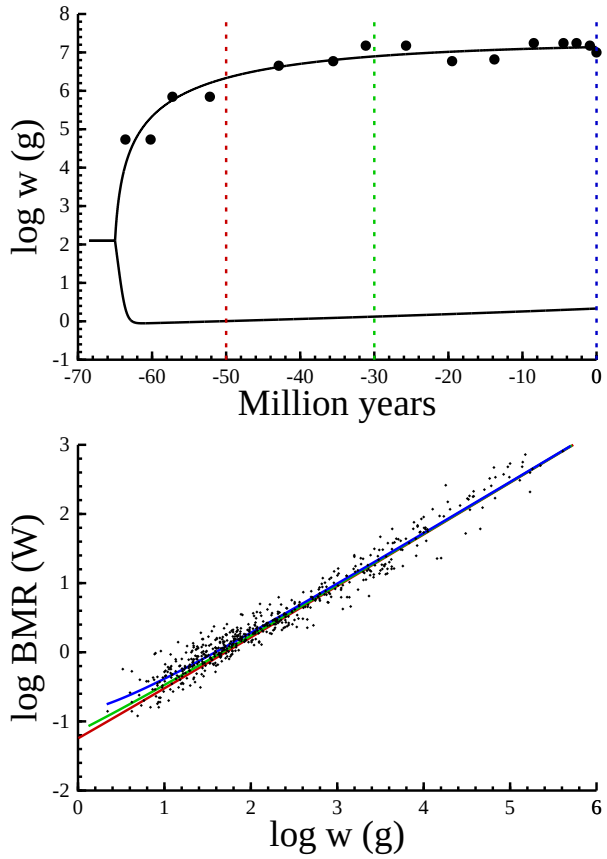

Figure 3: **Placental mammals. Top:** the span of the simulated body mass (w) distribution over time (curves), with dots being the global maximum estimates from Smith et al. (2010). The dashed colour lines mark the time of the simulated allometries in the bottom plot. **Bottom:** the simulated (colour curves) and observed (dots) relationship between the basal metabolic rate (BMR) and body mass (w). 50 million years ago (MA): red curve. 30MA: green curve. 0MA: blue curve and data dots from McNab (2008).

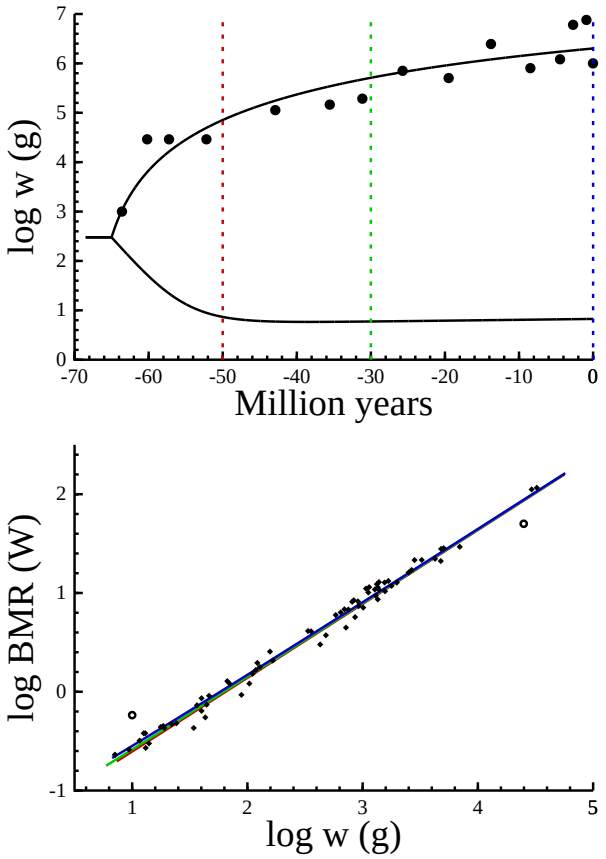

Figure 4: **Marsupial mammals. Top:** the span of the simulated body mass (w) distribution (curves), with dots being estimates of the maximum mass in South America from Smith et al. (2010). **Bottom:** the simulated (colour curves) and observed (dots) relationship between the basal metabolic rate (BMR) and body mass (w). Data from McNab (2008), with two outlier species (*Tarsipes rostratus* and *Lasiorhinus latifrons*) marked by open circles. See Fig. 3 and text for more details.

result is an inter-specific allometry that becomes more and more bent over time by the primary selection on mass-specific metabolism.

The best fit of the current allometry is given by the blue curve in the bottom plot. The upward bend in the metabolism of the smaller placental mammals implies that the overall exponent is smaller than 0.75, if approximated by a linear allometry that is fitted to the simulated data. The overall linear exponent is 0.72 across the entire range of simulated body masses, and it increases to 0.74 for the upper half of the body mass distribution, and declines to 0.67 for the lower half. The estimated rate of exponential increase in the pre-mass component of mass-specific metabolism (r_{β_β}) is 9.3×10^{-9} (95% CI: 7.3×10^{-9} - 1.1×10^{-8}) on the per-generation time-scale.

To examine whether the observed bend was caused mainly by the contrast between the largest and smallest placentals, I truncated the data to the range from 7 g to 32 kg so that it corresponded with the mass range in the marsupial data. This provided a slightly larger point estimate of 1.1×10^{-8} that shows that the bend is equally present in the middle range of the mass data for placentals.

Sensitivity analysis showed that the estimated r_{β_β} is invariant with respect to deviations in the mass of the ancestor. Yet, being a per-generation rate, the absolute value of r_{β_β} depends on the assumed generation

time, with an increase in the initial generation time by 20% generating an approximate 20% increase in the estimate.

3.2 Marsupial mammals

The simulated span of body masses for marsupial mammals over the past 65 million years are shown in the top plot in Fig. 4 for the best estimate of the exponential increase in metabolism, with the evolution of the inter-specific allometry shown in the bottom plot. The bend in marsupials is clearly smaller than in placentals, with the per-generation estimate of the exponential increase in the pre-mass component of mass-specific metabolism (r_{β_β}) being 3.1×10^{-9} (95% CI: 4.6×10^{-21} - 5.4×10^{-9}), given a current generation time of 2.9 years for a 309 grams marsupial.

This estimate is strongly dependent on the two outlier species that were identified by MacKay (2011). The estimate for r_{β_β} declines by almost an order of magnitude to 6.3×10^{-10} per-generation (95% CI: 4.2×10^{-22} - 2.9×10^{-9}) in the absence of the two species. Using 5.1 years as the target for the current generation time of a 309 grams marsupial, we obtain a r_{β_β} estimate of 1.0×10^{-9} per-generation (95% CI: 2.9×10^{-22} - 5.0×10^{-9}) with the two outlier species removed. This rate is approximately an order of magnitude smaller than the estimate for placentals.

4 Discussion

Hayssen and Lacy (1985) found the allometry for metabolism across the size range of mammals to be, not a straight line, but an upward bend curve that is better described by a second order polynomial. While a significant detection is dependent on phylogenetic effects and methods of analysis (Ehnes et al. 2011; MacKay 2011; Packard 2015; Griebeler and Werner 2016), a rather persistent presence in placentals (Hayssen and Lacy 1985; Kolokotrones et al. 2010; MacKay 2011) indicates a bend that is likely to reflect some underlying regularity in the natural selection of metabolism and mass.

Primary selection for a persistent increase in mass-specific metabolism indicates that it can be selected to an upper limit, in line with an allometric invariance on the macro-evolutionary scale from prokaryotes to mammals (Makarieva et al. 2005, 2008; Kiørboe and Hirst 2014). This suggests a macro evolution where the major taxonomic groups evolve along an upper bound on mass-specific metabolism (Witting 2017b), a result that is supported also by a log-linear increase in the maximum mass of mobile organisms over 3.5 billion years of evolution (Witting 2008, 2016).

While the maximum rates of mass-specific metabolism are rather similar across the major taxonomic groups, the majority of animals are not selected to the limit (Makarieva et al. 2005, 2008). Mass-rescaling selection is the likely cause for this, as it selects for a mass-specific metabolism that declines with the size increase that occurs in many species when a clade diversifies into a multitude of species. Following this diversification of mammals at the Cretaceous-Palaeogene boundary, and the associated selection of larger masses and smaller metabolic rates, I simulated the background selection of mass-specific metabolism in placentals and marsupials to estimate the degree of bending of the inter-specific allometry over time.

Models for vascular transportation systems in multicellular organisms have an inbuild curvature in the allometry between metabolism and mass (West et al. 1997; Kolokotrones et al. 2010). But this non-linearity is bend downward, instead of upward as observed. Kolokotrones et al. (2010), however, constructed modified vascular models to reflect an upward bend, and this indicates that the physiology is sufficiently flexible to allow for the evolution of the observed curvature.

I predicted the bend from the primary selection of mass-specific metabolism and found it to be more apparent in placentals than marsupials. This difference was estimated to reflect a per-generation rate of increase in mass-specific metabolism that is about one order of magnitude larger in placentals. From the differences in the curvature of the metabolic allometry, we conclude that placentals have evolved a higher metabolism than marsupials, in agreement with an average metabolism that is 30% larger in placentals relative to marsupials of similar size (McNab 2008).

The simulated selection of placentals produced an overall exponent of 0.72, if a linear allometry was fitted to the entire range of simulated masses. The estimated exponent increased to 0.74 for the upper half of the distribution, and declined to 0.67 for the lower half. This change coincides with the observed pattern (Kolokotrones et al. 2010), and it provides a mechanistic explanation for the 2/3 versus 3/4 controversy that has dominated the field of allometries for decades (Rubner 1883; Kleiber 1932; Heuser 1982; Feldman and McMahon 1983; Calder 1984; Dodds et al. 2001; White and Seymour 2003; Savage et al. 2004; Glazier 2010).

The selection of metabolism and mass predicts 3/4 as the primary exponent that evolves for 2D systems when phylogenetic clades diversify by speciation over a

multitude of ecological niches (Witting 2017a). The 2/3 exponent for the lower half of the distribution evolves instead as a secondary effect of a curvature that is selected over millions of years by the back-ground selection of mass-specific metabolism. Although all species may have a similar increase in mass-specific metabolism on the per-generation time-scale of natural selection, this selection generates increased metabolism in the smaller species in physical time as they evolve over a much larger number of generations than the larger species.

The primary selection of metabolism is not only generating the bend of the metabolic allometry, but it provides also a mechanism for the evolution of well-known allometric outliers. This is exemplified in Fig. 4 (bottom) by the small honey possum *Tarsipes rostratus* with a high metabolism, and the large southern hairy-nosed wombat *Lasiorhinus latifrons* with a low metabolism. This outlier pattern, with small species with high metabolism and large species with low metabolism, is seen also in placentals, where shrews (*Soricidae*) have an increased metabolism (Platt 1974) and bowhead whales *Balaena mysticetus* a smaller metabolism (George 2009) than expected from mass alone. This is predicted by the primary selection of metabolism and mass as a time response in lineages that evolve a small or large body mass at an early stage relative to the other species in the clade. They will then evolve over a larger or smaller number of generations that the main clade, and evolve a higher or lower metabolic rate.

There seems, however, to be a slight difference between the predicted and observed curvature. The selection of metabolism and mass that was simulated in this paper predicts 3/4 for 2D systems, and 5/6 for 3D systems, as the maximum exponents to be estimated by a linear model that is fitted to the upper range of the size distribution. Yet, the observed exponent in the upper range of mostly 2D placentals appears to be around 0.87 (Kolokotrones et al. 2010). This apparent increase in the metabolism of the larger species can evolve as an indirect consequence of the mass-rescaling selection that generates the -1/2d power decline in mass-specific metabolism with increased mass. This mass-rescaling implies smaller species with mass-specific metabolic rates that are much closer to an upper limit than the metabolism of larger species. It should therefore be easier to select for increased metabolism in the larger species, with a per-generation rate of increase (r_{β_β}) that is slightly larger in the larger species, instead of being mass invariant as assumed in this paper.

References

Banavar J. R., Maritan A., Rinaldo A. (1999). Size and form in efficient transportation networks. Nature 399:130–132.

Brown J. H., Gillooly A. P., Allen V. M., Savage G. B. (2004). Towards a metabolic theory of ecology. Ecology 85:1771–1789.

Brown J. H. Sibly R. M. (2006). Life-history evolution under a production constraint. Proc. Nat. Acad. Sci. 103:17595–17599.

Bueno J. López-Urrutia A. (2012). The offspring-development-time/offspring-number trade-off. Am. Nat. 179:E196–E203.

Calder W. A. I. (1984). Size, function, and life history. Harvard University Press, Cambridge.

Damuth J. (1981). Population density and body size in mammals. Nature 290:699–700.

Damuth J. (1987). Interspecific allometry of population density in mammals and other animals: the independence of body mass and population energy-use. Biol. J. Linnean Society. 31:193–246.

Dawkins R. Krebs J. R. (1979). Arms races between and within species. Proc. R. Soc. Lond. B. 205:489–511.

DeLong J. P., Okie J. G., Moses M. E., Sibly R. M., Brown J. H. (2010). Shifts in metabolic scaling, production, and efficiency across major evolutionary transitions of life. Proc. Nat. Acad. Sci. 107:12941–12945.

Dodds P. S., Rothman D. H., Weitz J. S. (2001). Re-examination of the "3/4-law" of metabolism. J. theor. Biol. 209:9–27.

Dreyer O. Puzio R. (2001). Allometric scaling in animals and plants. J. Math. Biol. 43:144–156.

Ehnes R. B., Rall B., Brose U. (2011). Phylogenetic grouping, curvature and metabolic scaling in terrestrial invertebrates. Ecol. Lett. 14:993–1000.

Feldman H. A. McMahon T. A. (1983). The 3/4 mass exponent for energy metabolism is not a statistical artifact. Resp. Physiol. 52:149–163.

Fenchel T. (1974). Intrinsic rate of natural increase: The relationship with body size. Oecologia 14:317–326.

George J. C. (2009). Growth, morphology and energetic of bowhead whales (*Balaena mysticetus*). (Thesis, Ph.D.). University of Alaska, Fairbanks.

Gillooly J. F., Charnov E. L., West G. B., Savage V. M., Brown J. H. (2002). Effects of size and temperature on developmental time. Nature 417:70–73.

Glazier D. S. (2010). A unifying explanation for diverse metabolic scaling in animals and plants. Biol. Rev. 85:111–138.

Griebeler W. M. Werner J. (2016). Mass, phylogeny, and temperature are sufficient to explain differences in metabolic scaling across mammalian orders? Ecol. Evol. 6:8352–8365.

Haigh J. Rose M. R. (1980). Evolutionary game auctions.

J. theor. Biol. 85:381–397.

Hayssen V. Lacy R. C. (1985). Basal metabolic rates in mammals: taxonomic differences in the allometry of bmr and body mass. Comp. Bioch. Physiol. 81A:741–754.

Heuser A. A. (1982). Energy metabolism and body zise, i. is the 0.75 mass exponent of kleiber's equation a statistical artifact? Resp. Physiol. 48:1–12.

Humphries M. M. McCann K. S. (2014). Metabolic constraints and currencies in animal ecology. metabolic ecology. J. Anim. Ecol. 83:7–19.

Kiørboe T. Hirst A. G. (2014). Shifts in mass scaling of respiration, feeding, and growth rates across life-form transitions in marine pelagic organisms. Am. Nat. 183:E118–E130.

Kleiber M. (1932). Body and size and metabolism. Hilgardia 6:315–353.

Kolokotrones T., Savage V., Deeds E. J., Fontana W. (2010). Curvature in metabolic scaling. Nature 464:753–756.

MacKay N. J. (2011). Mass scale and curvature in metabolic scaling. J. theor. Biol. 280:194–196.

Makarieva A. M., Gorshkov V. G., Bai-Lian L. (2005). Energetics of the smallest: do bacteria breathe at the same rate as whales. Proc. R. Soc. B. 272:2219–2224.

Makarieva A. M., Gorshkov V. G., Li B., Chown S. L., Reich P. B., Gavrilov V. M. (2008). Mean mass-specific metabolic rates are strikingly similar across life's major domains: Evidence for life's metabolic optimum. Proc. Nat. Acad. Sci. 105:16994–16999.

Maynard Smith J. Brown R. L. W. (1986). Competition and body size. Theor. Pop. Biol. 30:166–179.

McNab B. K. (2008). An analysis of the factors that influence the level and scaling of mammalian bmr. Comp. Bioch. Physiol. A 151:5–28.

O'Leary M., Bloch J. I., Flynn J. J., Gaudin T. J., Gillombardo A., Giannini N. P., Goldberg S. L., Kraatz B. P., Luo Z., Meng J., Ni X., Novacek M. J., Perini F. A., Randall I. Z. S., Rougier G. W., Sargis E. J., Silcox M. T., Simmons N. B., Spaulding M., Velazco P. M., Weksler M., Wible J. R., Cirranello A. L. (2013). The placental mammal ancestor and the post-k-pg radiation of placentals. Science 339:662–667.

Pacifici M., Santini L., Di Marco M., Baisero D., Francucci L., Marasini G. G., Visconti P., Rondinini C. (2013). Generation length for mammals. Nature Cons. 5:87–94.

Packard G. C. (2015). Quantifying the curvilinear metabolic scaling in mammals. J. Exp. Zool. 323A:540–546.

Packard G. C. Birchard G. F. (2008). Traditional allometric analysis fails to provide a valid perdictive model for mammalian metabolic rates. J. Exp. Biol. 211:3581–3587.

Parker G. A. (1979). Sexual selection and sexual conflict. In: Blum M. S. Blum N. A. (eds). Sexual selection and reproductive competition in insects: Academic Press, New York, pp 123–166.

Parker G. A. (1983). Arms races in evolution–an ess to the opponent-independent cost game. J. theor. Biol. 101:619–648.

Peters R. H. (1983). The ecological implication of body size. Cambridge University Press, Cambridge.

Platt W. J. (1974). Metabolic rates of short-tailed shrews. Physiol. Zool. 42:75–90.

Rau A. R. P. (2002). Biological scaling and physics. J. Biosci. 27:475–478.

Rubner M. (1883). Über den einfluss der korper grosse auf stoff-und kraft-wechsel. Z. Biol. 19:535–562.

Santillán M. (2003). Allometric scaling law in a simple oxygen exchanging network: possible implications on the biological allometric scaling laws. J. theor. Biol. 223:249–257.

Savage V. M., Gillooly J. F., Wooduff W. H., West G. B., Allen A. P., Enquist B. J., Brown J. H. (2004). The predominance of quarter-power scaling in biology. Funct. Ecol. 18:257–282.

Sibly R. M., Brown J. I., Kodric-Brown A. (2012). Metabolic ecology: A scaling approach. John Wiley & Sons, Chichester.

Simpson G. G. (1953). The major features of evolution. Columbia University Press, New York.

Smith C. C. Fretwell S. D. (1974). The optimal balance between size and number of offspring. Am. Nat. 108:499–506.

Smith F. A., Boyer A. G., Brown J. H., Costa D. P., Dayan T., Ernest S. K. M., Evans A. R., Fortelius M., Gittleman J. L., Hamilton M. J., Harding L. E., Lintulaakso K., Lyons S. K., McCain C., Okie J. G., Saarinen J. J., Sibly R. M., Stephens P. R., Theodor J., Uhen M. D. (2010). The evolution of maximum body size of terrestrial mammals. Science 330:1216–1219.

Stearns S. C. (1992). The evolution of life histories. Oxford University Press, Oxford.

Vermeij G. J. (1987). Evolution and escalation. Princeton University Press, Princeton.

West G. B., Brown J. H., Enquist B. J. (1997). A general model for the origin of allometric scaling laws in biology. Science 276:122–126.

West G. B., Brown J. H., Enquist B. J. (1999a). A general model for the structure and allometry of plant vascular systems. Nature 400:664–667.

West G. B., Brown J. H., Enquist B. J. (1999b). The fourth dimension of life: Fractal geometry and allometric scaling of organisms. Science 284:1677–1679.

White C. R., Blackburn T. M., Seymour R. S. (2009). Phylogenetically informed analysis of the allometry of mammalian basal metabolic rate supports neither geometric nor quarter-power scaling. Evolution 63:2658–2667.

White C. R. Seymour R. S. (2003). Mammalian basal metabolic rate is proportional to body mass$^{2/3}$. Proc. Nat. Acad. Sci. USA 100:4046–4049.

Witting L. (1995). The body mass allometries as evolutionarily determined by the foraging of mobile organisms. J. theor. Biol. 177:129–137.

Witting L. (1997). A general theory of evolution. By means of selection by density dependent competitive interactions. Peregrine Publisher, Århus, 330 pp, URL http://mrLife.org.

Witting L. (2000). Interference competition set limits to the fundamental theorem of natural selection. Acta Biotheor. 48:107–120.

Witting L. (2003). Major life-history transitions by deterministic directional natural selection. J. theor. Biol. 225:389–406.

Witting L. (2008). Inevitable evolution: back to *The Origin* and beyond the 20th Century paradigm of contingent evolution by historical natural selection. Biol. Rev. 83:259–294.

Witting L. (2016). The natural selection of metabolism bends body mass evolution in time. Preprint at bioRxiv http://dx.doi.org/10.1101/088997.

Witting L. (2017a). The natural selection of metabolism and mass selects allometric transitions from prokaryotes to mammals. Theor. Pop. Biol. 117:23–42, http://dx.doi.org/10.1016/j.tpb.2017.08.005.

Witting L. (2017b). The natural selection of metabolism and mass selects lifeforms from viruses to multicellular animals. Ecol. Evol. 7:9098–9118, http://dx.doi.org/10.1002/ece3.3432.